

# Numerical study of linear dissipative drift electrostatic modes in tokamaks

M. Romanelli<sup>a)</sup>

*Euratom/UKAEA Fusion Association, Culham Science Centre, OXON, OX14 3DB, United Kingdom*

G. Regnoli

*Associazione Euratom-ENEA sulla fusione, Via E. Fermi 44, 00045 Frascati, Italy*

C. Bourdelle

*Association Euratom-CEA DRFC, CEA/DSM/DRFC Cadarache 13108, Saint-Paul-Lez-Durance, France*

(Received 18 May 2007; accepted 15 June 2007; published online 8 August 2007)

The linear stability of dissipative drift electrostatic modes in tokamak plasmas is studied numerically with an extended version of the gyrokinetic code Kinezero [C. Bourdelle *et al.*, Nucl. Fusion **42**, 892 (2002)] including a modified Krook collision operator to account for collisional effects on the trapped electron response. This new version of Kinezero has been successfully tested and benchmarked against the results of a more sophisticated and complete gyrokinetic solver, GS2 [M. Romanelli, C. Bourdelle, and W. Dorland, Phys. Plasmas **11**, 3845 (2004)]. The critical density and temperature gradients for ion gradient driven modes (ITG) and trapped electron modes (TEM) have been computed for different values of collisionality. The threshold for TEM disappears as the collisionality increases. A detailed study of the dependence of the growth rate of the dissipative TEM on collisionality and density gradient is presented in the paper. The range of parameters where the dissipative trapped electron modes are destabilized by increasing collisionality corresponds to very steep density gradients that can hardly be achieved in today's large tokamaks. © 2007 American Institute of Physics. [DOI: [10.1063/1.2755981](https://doi.org/10.1063/1.2755981)]

## I. INTRODUCTION

The study of electrostatic drift instabilities in tokamaks has long been a key topic in fusion research.<sup>1</sup> It is commonly understood that anomalous transport in tokamaks is largely driven by electrostatic drift turbulence. Furthermore, transition phenomena such as the formation of internal transport barriers (ITB) or the low (L) to high (H) mode confinement transition are believed to be associated with local turbulence stabilization and subsequent improvement of the local thermal conductivity. Several physics mechanisms contribute to the stabilization of drift turbulence, such as the change of the magnetic shear, the increase of the  $E \times B$  (where  $E$  and  $B$  are, respectively, the electric and magnetic fields) shearing rate, changes in the zonal flows, and collisionality effects. In this paper, we analyze the effect of collisions on the stability of the drift electrostatic modes using the linear gyrokinetic code Kinezero,<sup>2</sup> which has been extended to include a Krook-type collision operator in the electron gyrokinetic equation. Electrostatic drift instabilities in toroidal plasmas have poloidal wave numbers  $k_\theta$  such that  $k_\theta \rho_i$  ranges from 0.1 up to  $10^3$  (where  $\rho_i$  is the ion Larmor radius). In particular, two subranges can be identified: long-wavelength modes ( $0.1 < k_\theta \rho_i < 2$ ), driven by the ion temperature gradient (ITG) and due to trapped electrons (TE modes), and short-wavelength modes ( $2 < k_\theta \rho_i < 10^3$ ), driven by the electron temperature gradient (ETG). The spatial structure of the dissipative TEM has been extensively investigated both analytically and numerically, for example in the case of a circular

cross section, large aspect ratio tokamak with concentric magnetic surfaces as in Ref. 3.

A recent analytic study of the dissipative trapped electron instability in steep density and temperature gradients, such as those found experimentally in internal transport barriers (ITBs) in the Mega Ampere Spherical Tokamak MAST,<sup>4</sup> shows that the growth rate of long-wavelengths TEM,  $k_\theta \rho_i < 0.5$ , has a non trivial dependence on collisionality. In particular, in the limit of low collisionality,  $\nu_{\text{eff}}/\omega \ll 1$ , where  $\nu_{\text{eff}} = \nu_{\text{ei}}/\varepsilon$  is the standard electron-ion collision frequency normalized to the inverse aspect ratio ( $\varepsilon = r/R$  is the inverse aspect ratio of a magnetic surface with minor radius  $r$  and major radius  $R$ ), the growth rate of the TEM is directly proportional to collisionality, while in the opposite limit  $\nu_{\text{eff}}/\omega \gg 1$ , the TEM are stabilized by increasing collisionality. The result of Ref. 4 shows that it is not possible to draw a general conclusion on the role of collisionality on drift instabilities, and whether it is a stabilizing or destabilizing contribution depends on plasma parameters and experimental profiles. In this paper, we will use Kinezero to study the dependence of TEM on collisionality and we will show that for realistic tokamak plasma parameters, TEM are stabilized by increasing collisionality.

The remainder of this work is organized as follows: in Sec. II, the collisional electron gyrokinetic equation and the benchmark with the results of another gyrokinetic code are presented; the stability limit of long-wavelength modes, computed at different collisionalities, is discussed in Sec. III; the scaling of the linear growth rate of the TEM with collisionality is discussed in Sec. IV; and Appendixes A and B give details of the most recent version of Kinezero.

<sup>a)</sup>Michele.Romanelli@ukaea.org.uk

## II. THE ELECTRON GYROKINETIC EQUATION

The ion linearized Vlasov equation remains unchanged, while we have included a Krook-type collision operator in the linearized Vlasov equation for the electron perturbed distribution function  $f_{1,e}$  such that

$$\frac{\partial f_{1,e}}{\partial t} + [f_{1,e}, H_{0,e}] + [f_{0,e}, H_{1,e}] = -\nu_{fe} \left( f_{1,e} - \frac{H_{1,e}}{T_e} f_{0,e} \right), \quad (1)$$

where  $f_{0,e}$  is the equilibrium Maxwellian distribution,  $H_{0,e}$  and  $H_{1,e}$  are, respectively, the equilibrium and the perturbed Hamiltonian ( $H_{1,e} = -e\tilde{\phi}$ , electrostatic fluctuations), and  $T_e$  is the electron temperature. The collision frequency as introduced in Ref. 5 is

$$\nu_{fe}(E, \lambda) = \nu_{ei} \left( \frac{v_{th}}{v} \right)^3 Z_{\text{eff}} \left( \frac{r/R}{|1 - r/R - \lambda|^2} \frac{0.111\delta + 1.31}{11.79\delta + 1} \right), \quad (2)$$

where  $\nu_{ei}$  is the electron-ion Coulomb collision frequency,  $\lambda$  is the pitch angle,  $v_{th}$  is the electron thermal speed, and  $\delta = [|\omega| / (\nu_{ei} Z_{\text{eff}} \times 37.2R/r)]^{1/3}$  with  $\omega$  the frequency of the unstable mode. The properties of the above collision operator and the numerical values appearing in Eq. (2) and in the definition of the parameter  $\delta$  are discussed in Ref. 5, the latter having been obtained by matching the solutions of the dispersion relation of Eq. (1) for the perturbed electron distribution function with analytical results and results obtained using a Lorentz collision operator. We have neglected the impact of collisionality on passing electrons assuming the limit  $k_{\parallel} v_{\parallel} \gg \nu_{fe}$ . Collisionality effects on the ion population have not been taken into account in the ordering  $\nu_{ii} \ll \nu_{ei}$ . Electron-electron collisions have also been neglected, however they would give a correction to  $Z_{\text{eff}}$  in the expression for  $\nu_{fe}$  which is negligible for the  $(v/v_{th}) \ll 1$  ordering.<sup>6</sup> We will consider electrons in the banana regime,  $\nu_{fe} \ll \omega_{be}$  (where  $\omega_{be}$  is the electron bounce frequency). We point out that although Eq. (1) does not conserve momentum and energy, the fraction of trapped electrons remains unchanged in the banana regime approximation. Furthermore, Eq. (1) has the conceptual advantage that, in the limit of high collisionality, it predicts a perturbed density equal to the density of a perturbed Maxwellian distribution. This can be seen by taking the first moment of Eq. (1) in the limit of infinite  $\nu_{fe}$ . In large aspect ratio tokamaks, trapped electrons exist in a portion of the velocity space proportional to  $\delta\lambda \approx \varepsilon$ . The factor  $\varepsilon = r/R$  in the definition of  $\nu_{fe}$  accounts for the fraction of trapped particles: the smaller the number of trapped particles is, the smaller is the effect of collisions on mode stability. The denominator  $|1 - r/R - \lambda|^2$  takes into account the particles that are barely trapped and belong to the boundary layer of velocity space between the trapped and passing populations. When  $\lambda$  is finite and close to  $(1 - \varepsilon)$ , the collision operator becomes large, thus giving a higher weight to the small population of electrons at the boundary between trapped and passing particles as they are expected to play an important role in weak collisionality regimes.<sup>7</sup> The last factor in the parentheses (depending on  $\delta$ ) is a further correction to

the collision operator for  $\nu_{\text{eff}}/\omega \ll 1$ . Substituting the perturbed distribution function calculated from Eq. (1) in the variational form of the quasineutrality condition as illustrated in Ref. 2, one obtains the following dispersion relation:

$$D(\omega) = \sum_s \frac{n_s Z_s^2}{T_s} [1 - L_{ts}(\omega) - L_{ps}(\omega)] = 0, \quad (3)$$

where  $L_{ts}$  and  $L_{ps}$  are, respectively, the functional expressing both adiabatic and resonant responses of trapped and passing particles of the species  $s$ .<sup>2</sup> Although Kinezero can handle two ion species, in this paper we will assume  $Z_{\text{eff}} = 1$ , therefore  $s = e, i$ . By carrying out the calculation, we find that the collision modified nonadiabatic response of trapped electrons in Eq. (3) is

$$L_{te} = \left\langle \int \frac{dk_r}{2\pi} J_0^2(k_{\perp} \rho_e) J_0^2(k_r \delta_e) \frac{\omega - n\omega_e^*}{\omega - n\omega_{de} + i\nu_{fe}} |\tilde{\phi}(k_r)|^2 \right\rangle_i, \quad (4)$$

where  $J_0^2(k_{\perp} \rho_e)$  and  $J_0^2(k_r \delta_e)$  are the Bessel functions representing the gyro-average over the electron cyclotron and the bounce motion, respectively. The term  $n\omega_{de}$  is the vertical drift frequency, the effect of collisions appears as an extra term in the denominator, and  $\omega_e^*$  is the diamagnetic electron frequency. The average implies an integral over the electron energy and pitch angle, which is calculated numerically in the code. The electrostatic potential  $\tilde{\phi}(k_r)$  is a trial function taken as the most unstable solution of the dispersion relation in the fluid limit for strongly ballooning modes.<sup>2</sup> An improved trial eigenfunction has been implemented recently in Kinezero in order to account for low magnetic shear cases (see Appendix A). Further corrections accounting for finite Larmor radius effects on integral (4) are reported in Appendix B. We point out here that the collisional operator has not been included in the ion gyrokinetic equation, therefore the ion response in the present version of the code remains that described in detail in Ref. 2 along with the response of passing electrons. The adoption of a Krook collision operator in the electron gyrokinetic equation in Kinezero allows one to preserve the characteristic speed of the code, hence carrying out a fast estimate of the effect of collisions on the growth rate and extensive parameter scans. Early analytical works carried out with the original Krook operator show that it can qualitatively describe the scaling of the linear growth rate of unstable modes with collisionality. The results obtained with the modified Krook operator can be eventually double-checked against a complete gyrokinetic code implementing the Lorentz operator, such as GS2.<sup>8</sup> We have verified that, in the limit of zero collisionality, the output of the code is not changed. Furthermore, the new version of the code has been benchmarked against results from the gyrokinetic code GS2, at different collisionalities and different values of the normalized logarithmic density gradient  $A_n = R/L_n$ , with  $L_n = -n/\nabla n$ .

In Ref. 8, it was shown that at high collisionality ( $\nu_{\text{eff}}/\omega \gg 1$ ), the density gradient has a stabilizing effect for low  $k_{\theta} \rho_i$  modes, whereas at low collisionality the effect is opposite. We have repeated the calculation with the new ver-

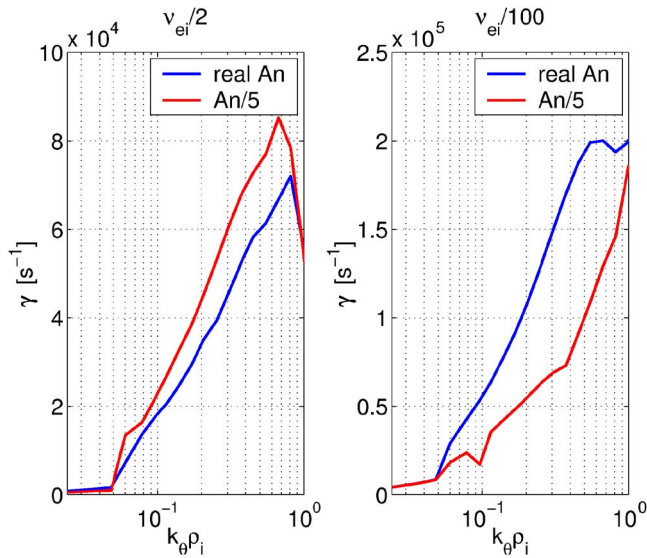


FIG. 1. (Color online) Maximum growth rate vs  $k_\theta \rho_i$  for two values of the density gradient ( $A_n$ ) and of the collision frequency ( $\nu_{ei}$ ), parameters of FTU no. 12747 at 0.7 s and  $r/a=0.7$  as in Ref. 8.

sion of Kinezero. The results are reported in Fig. 1, where the largest linear growth rate,  $\gamma$ , is plotted as a function of  $k_\theta \rho_i$  at the radial position  $r/a=0.7$ , for two values of  $A_n$  and at two different collisionalities. In Fig. 1, we find the same result as Ref. 8: an opposite effect of increased density gradient at high and low collisionality. The values of the linear growth rate calculated with Kinezero are slightly lower than those calculated with GS2, as can be found by comparing Fig. 1 with Fig. 8 of Ref. 8.

### III. THE STABILITY LIMIT

Kinezero solves the dispersion relation Eq. (3),  $D(\omega) = 0$ , in the complex plane (solutions of the form  $\omega = \omega_r + i\gamma$ ) for any given radial position  $r$  and wave number  $k_\theta \rho_i$ . We have used the solver to compute the stability thresholds of long-wavelength modes in the  $(A_n, A_T)$  plane, namely to find the solutions of Eq. (3) within a fixed range of mode frequencies  $\omega_1 < \omega_r < \omega_2$  and  $\gamma \approx 0^+$ . We have taken the normalized gradients  $A_{Ti} = R/L_{Ti} = A_{Te} = R/L_{Te} = A_T$ ,  $T_e = T_i$ ,  $A_{ne} = A_{ni} = A_n$ ; magnetic shear  $s$  is chosen such that the vertical drift frequency of trapped and passing particles is equal to  $n\omega_{ds} = k_\theta T_s / (e_s BR)$ , and we have neglected Shafranov shift effects (in particular, we have taken  $\alpha = 0$ ,  $\alpha$  being the magnetohydrodynamic (MHD)  $\alpha = -Rq^2(d\beta/dr)$ ). The results, obtained for typical tokamak plasma parameters and for modes with  $k_\theta \rho_i = 0.4$ , are plotted in Fig. 2. Here the collisionality is taken into account through the nondimensional parameter

$$A_\nu = \frac{\nu_{ei} Z_{\text{eff}}^2 BR}{k_\theta T_e} \left( \frac{r/R}{|1 - r/R - \lambda|^2} \frac{0.111\delta + 1.31}{11.79\delta + 1} \right), \quad (5)$$

which is proportional to the effective collision frequency  $\nu_{fe}$ . In highly collisional plasmas, the parameter  $A_\nu$  can exceed  $10^7$  while for typical JET (Joint European Torus) discharges,  $A_\nu = 10^4 - 10^5$ . Figure 2 shows that by increasing the collisionality, the area of the  $(A_n, A_T)$  plane where both the ITG and the TEM are unstable shrinks and the TEM are no longer

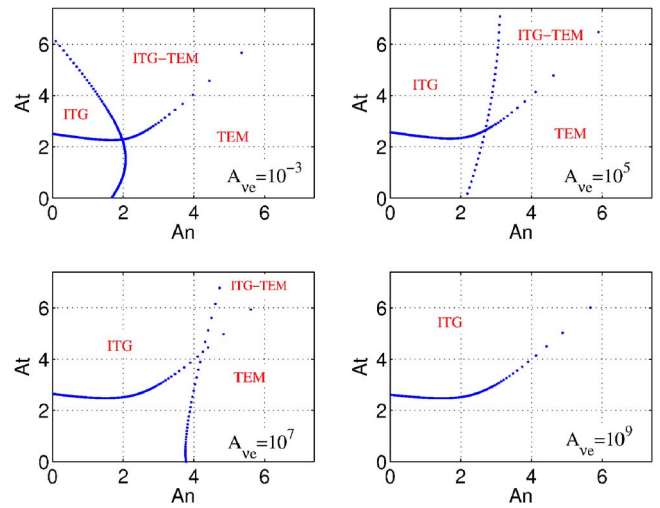


FIG. 2. (Color online) ITG, TEM stability threshold in the plane  $(A_n, A_T)$  for different values of the collisional parameter  $A_\nu$ .

destabilized by high-temperature gradients  $A_T$ , but only by high values of the density gradient  $A_n$ . For  $A_\nu \geq 10^9$ , the TEM become stable for any values of the density and temperature gradient and only the ITG can be destabilized. The numerical result confirms that TEM instabilities are not affecting the confinement properties of highly collisional plasmas where in general the contribution of trapped electrons is less important; this result could have been anticipated by noting that the denominator of Eq. (3) becomes infinite for high collisionalities. It is important to point out that the stability diagrams of Fig. 2 are calculated for a given set of plasma parameters and within certain assumptions. For the purpose of comparing with experiments, Fig. 2 can be taken as a qualitative description of the parametric behavior of the stability limit, but it cannot replace a dedicated stability analysis carried out with the exact plasma parameters of a given discharge.

### IV. TEM GROWTH RATE SCALING WITH COLLISIONALITY

In this section, we focus on the stability of TEM in collisional plasmas. As was shown by Kadomtsev and Pogutse,<sup>10</sup> the TEM can be either destabilized or stabilized by collisionality, and the scaling of the linear growth rate with collisionality depends on the frequency range of the mode itself. In early studies of the dissipative TEM, the kinetic equation with a Krook operator was linearly solved. Those models predicted unstable trapped electron modes with a growth rate  $\gamma \propto \omega / \nu_{\text{eff}}$  in the range of  $\nu_{\text{eff}} / \omega \gg 1$ . In the opposite limit ( $\nu_{\text{eff}} / \omega \ll 1$ ), the growth rate was found to scale as  $\gamma \propto (\omega / \nu_{\text{eff}})^{-1}$ , indicating that the TEM can be destabilized by increasing collisionality. Recently, Connor *et al.*<sup>4</sup> have obtained a more accurate analytical expression for the growth rate of long-wavelength TEM, in the two above-mentioned frequency limits by investigating the effect of collisionality in the presence of steep density gradients (in particular,  $A_n = R/L_n = 50$ ) and using a pitch angle scattering operator for modeling the effect of collisions. In Ref. 4, it is

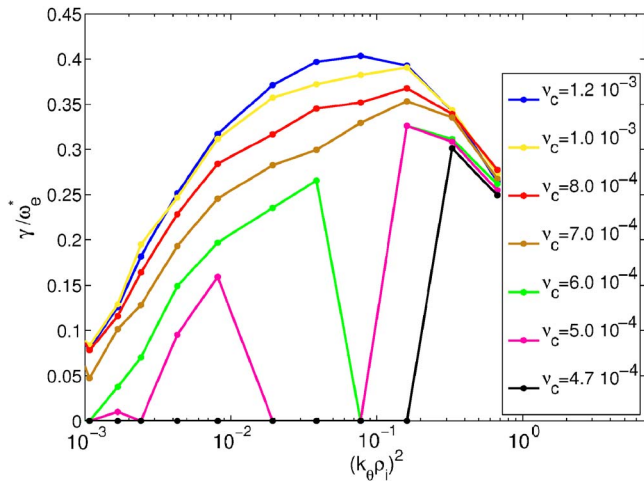


FIG. 3. (Color online) Maximum growth rate vs  $k_{\theta}\rho_i$  for seven different values of  $\nu_c$  and plasma parameters such that  $\nu_{\text{eff}}/\omega \ll 1$ .

found that for  $\nu_{\text{eff}}/\omega \ll 1$ , the linear growth rate of TEM is proportional to the nondimensional parameter  $\nu_c = \nu_{ei} L_n / V_{th}$ . We have used Kinezero to study the dependence of the growth rate of the long-wavelength TEM on  $\nu_c$ . Thanks to the implementation of the modified Krook collisional operator (see Sec. I), the different scalings of the growth rate with collisionality in the two frequency limits are captured by the code. The growth rate versus  $k_{\theta}\rho_i$  for seven different values of  $\nu_c$  and for plasma parameters such that  $\nu_{\text{eff}}/\omega \ll 1$  is plotted in Fig. 3. The following set of plasma parameters has been assumed:  $T_e = T_i = 1$  keV,  $Z_{\text{eff}} = 1$ ,  $\eta_i = 0$  and  $\eta_e = 1$ ,  $\varepsilon = 0.2$ ,  $q = 2$ ,  $s = 1$ , and  $n_e = 10^{18}$  m $^{-3}$ . Here we have set  $\eta_i = 0$  (instead of  $\eta_i = \eta_e = 1$  as in Ref. 4) in order to exclude ITG instabilities from the solutions calculated by Kinezero. We see from Fig. 3 that the increase in collisionality has a destabilizing effect on long-wavelength electrostatic modes. Indeed, the TEM growth rate increases with  $\nu_c$  in agreement with the analytical result for the low collisionality regime  $\nu_{\text{eff}}/\omega \ll 1$ .

However, we point out that in Ref. 4, the above scaling is found for  $10^{-3} < \nu_c < 2 \times 10^{-2}$  whereas we observe the same dependence for lower values of  $\nu_c$ , that is, for  $\nu_c \leq 10^{-3}$ . Figure 4 illustrates the change in the growth rate at  $k_{\theta}\rho_i = 0.2$  as a result of a scan of  $\nu_c$  obtained by varying  $L_n$ . The growth rate increases up to a maximum, corresponding to a critical value of  $\nu_c$ , followed by an inversion of the trend. For this set of plasma parameters, the maximum growth rate is obtained for  $\nu_c = 1.5 \times 10^{-3}$ . For large  $L_n$  (corresponding to reduced density gradients  $A_n$ ), the condition  $\nu_{\text{eff}}/\omega \gg 1$  is satisfied and increasing  $\nu_c$  has a stabilizing effect. The value  $\nu_c = 1.5 \times 10^{-3}$  corresponds to  $A_n = R/L_n = 8$ . Since  $\nu_c$  is inversely proportional to  $A_n$ , we find that the range of parameters where the TEM are destabilized by collisionality corresponds to steeper density gradients that can hardly be achieved in large tokamaks, e.g., JET discharges. Indeed, the normalized density gradient value of typical JET ITB discharges does not exceed values of  $A_n = 6-7$ . Hence, we find that for standard JET conditions, collisions always have a stabilizing effect on the TEM, unless very large den-

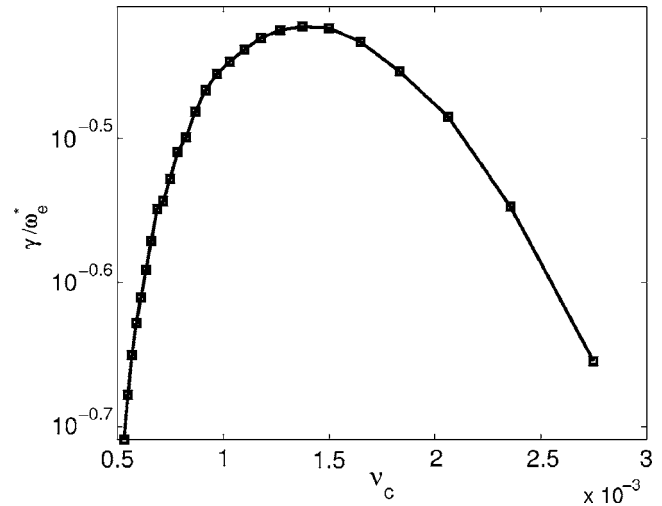


FIG. 4. Maximum growth rate vs  $\nu_c$  for long-wavelength modes with  $k_{\theta}\rho_i = 0.2$ . The increasing values of  $\nu_c$  have been obtained by varying  $L_n$ .

sity gradients are reached, in which case dissipative electron modes can be destabilized by collisions.

In the presence of very steep density gradients, (e.g.,  $A_n = R/L_n > 50$  as is assumed in Ref. 4), the Landau drift-resonant drive, which is responsible for the collisionless TEM growth rate, is negligible in the limit of long-wavelength modes  $k_{\theta}\rho_i \ll 1$ , and the term  $n\omega_{de}$  can be neglected as compared to  $\omega$  in the denominator of Eq. (4), while in standard tokamak plasmas the Landau drift-resonant effects remain important. This can explain the different range for the parameter  $\nu_c$  at which the effect of collisional destabilization of the TEM is found in this paper as compared to Ref. 4. Taking into account the Landau drift resonance, we expect to recover the result of Ref. 4 for  $\nu_c = \nu_c^* - n\omega_{de}$ , where  $\nu_c^*$  is the value of the collision frequency of Ref. 4. Differences between Kinezero and the analytic result of Ref. 4 can arise as well from the presence of a magnetic shear dependence for the TEM in Kinezero.

## V. CONCLUSION

Collisions have been introduced in the linear gyrokinetic code Kinezero by adding a modified Krook operator in the electron gyrokinetic equation. The output of this new version of Kinezero has been successfully benchmarked against calculations carried out with the GS2 code. The threshold gradients for the stability of electrostatic drift modes at different collisionalities have been computed, and it has been shown that the threshold for the TEM on the plane  $(A_n, A_T)$  varies considerably: as collisionality increases, the TEM can be destabilized only by steep density gradients up to a critical value of the collision frequency when the TEM become completely stable. The ITG threshold remains unchanged. We have also studied the scaling of the growth rate of long-wavelength modes with collisionality focusing on the TEM. The scaling of the growth rate of the TEM with collisions has been successfully compared with the analytical results of Connor *et al.*, where it is found that for increasingly steeper density gradients, dissipative trapped electron modes can be

stabilized. Nevertheless, it has been shown that for typical JET plasma parameters, the value of  $R/L_n$ , which increases during the formation of an internal transport barrier, remains still too low to stabilize these modes. In general, for typical tokamak parameters, collisions have a stabilizing effect on TEM.

## ACKNOWLEDGMENTS

The authors would like to thank Dr. J. Connor, Dr. J. Hastie, and Dr. P. Helander for fruitful discussions on the results presented in this paper. The authors would also like to thank Dr. R. Waltz and Dr. J. Candy for providing the gyrokinetic code GYRO and Dr. W. Dorland for providing the gyrokinetic code GS2.

This work was funded jointly by the United Kingdom Engineering and Physical Sciences Research Council and by the European Communities under the contract of Association between EURATOM and UKAEA and under the contract of Association between EURATOM and ENEA. The views and opinions expressed herein do not necessarily reflect those of the European Commission.

## APPENDIX A: IMPROVED TRIAL EIGENFUNCTION IN KINEZERO

Kinezero is a numerical tool that enables one to find the eigenvalues of the dispersion relation (4) using the distribution functions calculated from the linearized gyrokinetic equation of the various particle species and assuming a trial eigenfunction for the electrostatic fluctuating potential. In other codes such as GS2 or GYRO,<sup>11</sup> both the eigenfunctions and the eigenvalues are calculated. The choice made for the trial eigenfunction in Kinezero has been presented and discussed in Ref. 2. The original choice for the trial eigenfunction prevents the investigation of low or zero magnetic shear plasma conditions. It is found that a simple modification of the trial function allows one to retain the correct dependency of the mode width,  $w$ , on the magnetic shear  $s$ , even for low values of  $s$ . The correction has been worked out by studying the electric field potential calculated with both the GYRO and GS2 codes varying the shear parameter  $s$ . In Kinezero, the width of the original trial eigenfunction was obtained by assuming that the parallel dynamic is balanced by the finite Larmor radius effects and considering the interchange mode to be the dominant instability. In particular, the width  $w$  was independent of  $s$  (see Ref. 2) assuming the ballooning limit  $\theta=0$ . However, in such a case, in the regions of low magnetic shear (where  $s$  goes to zero), the distance between the rational surfaces  $d$  became much larger than the mode width  $w$ . Hence, where the magnetic shear is small, the ballooning approximation fails. We have removed this limitation of the code considering the limit  $\theta \rightarrow 0$  rather than strictly setting  $\theta=0$ . In this case, the vertical drift frequency  $n\omega_{ds}$  in the balance equation has the following expression:

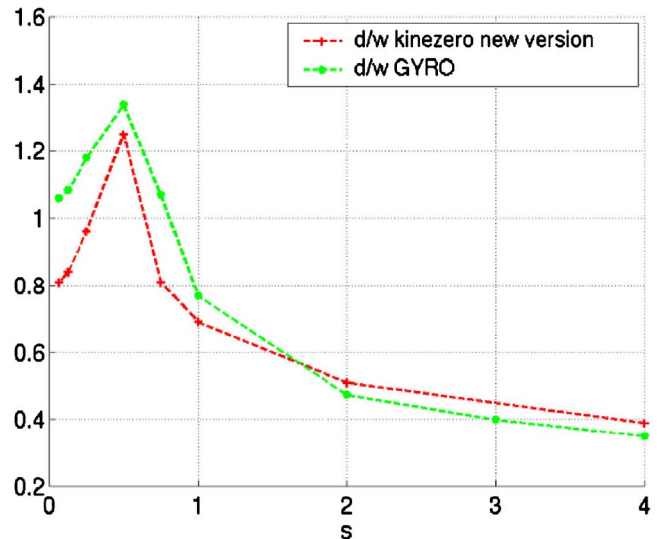


FIG. 5. (Color online) Comparison of the  $d/w$  ratio dependence on the magnetic shear for the eigenfunctions calculated with GYRO and those used in Kinezero.

$$n\omega_{ds} = \frac{-k_{\theta}T_s}{e_s BR} (\cos \theta + s\theta \sin \theta) \rightarrow \frac{-k_{\theta}T_s}{\theta \rightarrow 0 e_s BR} \times [1 + \theta^2(s - 0.5)].$$

It can be shown that the width  $w$  dependence on the magnetic shear  $s$  becomes

$$w^4 \rightarrow \frac{1}{s^2} + \frac{C_{Te}(s - 0.5)}{s^4},$$

where the sound speed  $C_{Te}$  is constant. In this limit, there is no divergence of the ratio  $d/w$  of the distance between resonant surfaces  $d$  over the mode width  $w$  when  $s \rightarrow 0$ . Using the expression above, the trial eigenfunction width used in Kinezero now shows a good agreement with the eigenfunctions from the GYRO code as is shown in Fig. 5.

## APPENDIX B: FINITE LARMOR RADIUS CORRECTIONS

The underestimation of the growth rates often found with Kinezero as compared to the results of GS2 (see the benchmark reported in Ref. 2) is due to the simplified way of accounting for both the finite Larmor radius effects and the bounce average. As detailed in Appendix A.4 of Ref. 2, the integration over energy in the Bessel functions originating from the gyro-average and bounce average is performed separately for both trapped and passing particles. Moreover, for trapped particles (electrons in particular), the bounce frequency is ordered larger than the other characteristic frequency and is neglected in the denominator of Eq. (3). The integration of the Bessel functions with respect to the energy leads to the appearance of terms of the form

$$B(a) = \int_0^{\infty} \frac{2}{\pi} \sqrt{\varepsilon} \exp(-\varepsilon) d\varepsilon J_0^2(a\varepsilon).$$

For mode wavelengths below either the Larmor radius  $\rho_s$  or the banana width  $\delta_s$ , the particles do not contribute to the

resonances. The analytic behavior of the Bessel functions integrated over energy correctly models this effect by decreasing exponentially for either  $k_{\perp} > \rho_s^{-1}$  or  $k_r > \delta_s^{-1}$ . In GS2 and GYRO, the integrals in energy of the Bessel functions are calculated numerically and the energy dependence of the bounce frequency is kept in the denominator and integrated as well. It turns out that the approximations made in Kinezero overestimate the finite Larmor radius and finite banana width effects. We have modified the arguments of the Bessel functions in Kinezero to correct this defect. For the trapped ions, the function  $B(k_r, \delta_i^{\text{th}})$  becomes  $B(k_r, \delta_i^{\text{th}}/20)$  and for the trapped electrons it becomes  $B(k_r, \delta_e^{\text{th}}/10)$ . For all passing particles,  $B(k_{\perp} \rho_{cs}^{\text{th}})$  becomes  $B(k_{\theta} \rho_{cs}^{\text{th}})$ .

<sup>1</sup>W. M. Tang, Nucl. Fusion **18**, 1089 (1978).

<sup>2</sup>C. Bourdelle, X. Garbet, G. T. Hoang, J. Ongena, and R. V. Budny, Nucl. Fusion **42**, 892 (2002).

<sup>3</sup>G. Rewoldt, W. M. Tang, and E. A. Frieman, Phys. Fluids **20**, 402 (1977).

<sup>4</sup>J. W. Connor, R. J. Hastie, and P. Helander, Plasma Phys. Controlled Fusion **48**, 885 (2006).

<sup>5</sup>G. Rewoldt, W. M. Tang, and M. S. Chance, Phys. Fluids **25**, 480 (1982).

<sup>6</sup>M. Kotschenreuther, G. Rewoldt, and W. M. Tang, Comput. Phys. Commun. **88**, 128 (1995).

<sup>7</sup>M. N. Rosenbluth, D. Ross, and D. P. Kostomarov, Nucl. Fusion **12**, 3 (1972).

<sup>8</sup>M. Romanelli, C. Bourdelle, and W. Dorland, Phys. Plasmas **11**, 3845 (2004).

<sup>9</sup>M. Keilhacker, A. Gibson, C. Gormezano, and P. H. Rebut, Nucl. Fusion **41**, 1925 (2001).

<sup>10</sup>B. B. Kadomtsev and O. P. Pogutse, Nucl. Fusion **11**, 67 (1971).

<sup>11</sup>J. Candy and R. E. Waltz, Phys. Rev. Lett. **91**, 045001 (2003).